Available online at www.sciencedirect.com

ScienceDirect

Acta Materialia 84 (2015) 359–367

Acta MATERIALIA

www.elsevier.com/locate/actamat

Local dislocation creep accommodation of a zirconium diboride silicon carbide composite

M.W. Bird,[a,*] T. Rampton,[b] D. Fullwood,[b] P.F. Becher[c] and K.W. White[a]

[a]*Department of Mechanical Engineering, University of Houston, Houston, TX, USA*
[b]*Department of Mechanical Engineering, Brigham Young University, Provo, UT, USA*
[c]*Department of Materials Science and Engineering, University of Tennessee, Knoxville, TN, USA*

Received 30 June 2014; revised 16 October 2014; accepted 16 October 2014
Available online 26 November 2014

Abstract—A grain boundary sliding creep mechanism, accommodated by "mantle" dislocation activities, is shown to allow for large strain ($\varepsilon > 0.08$) during the creep of a ZrB_2–20% SiC composite at 1800 °C. We characterized the local grain deformation behavior using high-resolution electron backscatter diffraction microscopy and an indentation deformation mapping technique. Deformation gradients near grain boundaries ("mantle") produced geometrically necessary dislocation (GND) densities of 1×10^{11}–1×10^{12} cm^{-2}, about two orders of magnitude above that of the grain interiors ("core"). A deviation from single-crystal grain core deformation defines the mantle where excess GNDs accommodate the grain deformation gradient. Evidence supporting grain boundary sliding as the primary contribution to the creep strain appears in our earlier publication, but we show here the role of dislocations in the deformation of the grain mantle as the rate-controlling accommodation step.

Keywords: Zirconium diboride; Creep; Grain boundary sliding; Dislocations; EBSD

1. Introduction

Extreme temperature environments ($T > 1500$ °C) require metal or metal compounds with melting points greater than 3000 °C [1,2]. A survey of materials meeting this one requirement limits the list to precious refractory metals, oxide, boride, carbide and nitride ceramic systems. Group IV borides, select group IV and V carbides and nitrides meet the high melting point criteria for such extreme environments [1–3]. Zirconium diboride compounds offer a unique combination of high melting points, high thermal conductivity, low density and thermodynamic stability, which make such materials candidates for aerodynamic applications ranging in temperature between 1500 and 2200 °C in oxidizing environments. Mechanical behavior transitions are to occur from predominately linear elastic to viscoplastic behavior. ZrB_2–20% SiC bending creep experiments conducted between 1400 and 1800 °C identified two distinct material behaviors: for $T < 1500$ °C diffusion creep and grain boundary sliding, while beyond 1600 °C grain boundary sliding at increased steady state strain rates of 10^{-9}–10^{-5} s^{-1} were observed [4]. Continued creep research on these composites has shown large accumulated macroscopic creep strains (>10%) with <10% cavitation leaving the post-creep microstructure very similar to its initial state. This, along with relatively low stress exponents, has focused our attention toward grain boundary sliding models, linked with a necessary dislocation accommodation process.

Langdon [5] proposed grain boundary sliding as an independently operating creep mechanism while maintaining a constant shape [5,6]. Later, Ashby and Verrall [35] proposed a two-dimensional neighbor-switching model with diffusion creep accommodating the small grain shape changes necessary for the sliding event. Gifkins [7,8] expanded on this notion, considering dislocation accommodation within a "mantle" region of the grain while leaving the "core" relatively free of dislocation activity. Combinations of grain boundary sliding and any affiliated rotations were needed for maintaining microstructural continuity while permitting large relative grain translations. A slip-dominated deformation process with increasing stress decorates the mantle zone with both statistically stored dislocations (SSDs) as well as geometrically necessary dislocations (GNDs) to satisfy the deformation compatibility requirements with the grain core [7]. This model promotes increased GND (mantle) importance with decreasing grain size. Both models require an increased mobile dislocation density in the mantle boundary over that of the grain core. This accommodation event will be shown to involve local grain deformations of the order of grain geometric parameter, y, as shown in Fig. 1.

* Corresponding author. Tel.: +1 2816306007, +1 2813636439; e-mail addresses: bird.marc@gmail.com; marc.bird@bakerhughes.com

http://dx.doi.org/10.1016/j.actamat.2014.10.037
1359-6462/

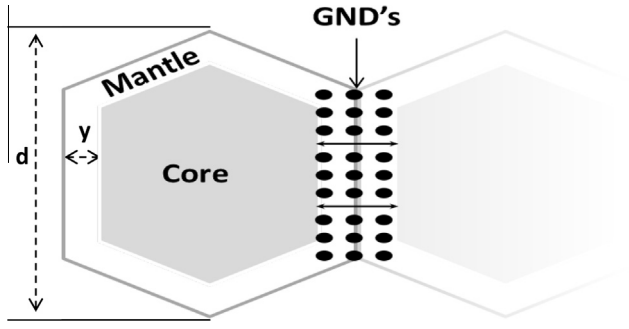

Fig. 1. Illustration of mantle–core grain deformation and the position of GNDs required for continuity, from the inherent deformation gradient. Recreated from Ref. [7]. Dimensions d and y are the grain size and mantle thickness, respectively.

Polycrystalline materials are plastically inhomogeneous, causing incompatible deformation between grains oriented with different critical resolved shear stresses or the presence of a second phase [9]. GNDs are required for microstructure compatibility in addition to the accumulating SSDs. Both SSD and GND dislocations can be individually inspected using transmission electron microscopy [10]. However, such studies typically cover a tiny specimen area, and sample preparation can remove or modify many of the defects being studied. At a higher length scale, X-ray techniques are often used for quantifying the GND densities of a plastically deformed polycrystal. These methods rely upon a continuum field of dislocations. At a given length scale, the net effect of GNDs within a virtual Burgers circuit distorts the crystal lattice. The rotational component of this distortion is then measured, and the GND content inferred; SSDs provide no net contribution to the distortion. However, the spatial resolution of the X-ray techniques is of the order of several microns, and is therefore not suitable for the more detailed study required for this paper.

On the other hand, electron backscatter diffraction (EBSD) and post processing orientation imaging microscopy (OIM) routines provide a higher resolution view of the GND fields [11–14]. These methods characterize the Kikuchi pattern distortion relative to a perfect, strain-free pattern of the same orientation, or relative to a pattern from elsewhere on the specimen [12,13]. For polycrystalline materials the GND density tensor is calculated based on Nye's relationship following [15,16]:

$$\alpha_{ik} = e_{jlk}\left(\frac{\partial \beta_{ij}}{\partial x_l}\right) = \nabla \times \beta \tag{1}$$

where the dislocation tensor α_{ik}, defined to be the curl of the elastic distortion tensor $\beta_{ij} = \frac{\partial u_i}{\partial x_j}$, includes both rigid rotation and strain components [12,14] e_{jlk} is the Levi–Civita symbol (or permutation tensor), and the usual Einstein summation convention is observed for repeated indices within a given term. The GND density on a given slip system, $\rho^{(m)}$, contributes to the total Nye tensor via the equation: $\alpha_{ij} = \sum_m \rho^{(m)} b_i^{(m)} v_j^{(m)}$, where b is the relevant Burgers vector and v is the corresponding unit vector in the line direction. Since OIM is a surface characterization technique, the derivatives required for Eq. (1) are only available in the 1 and 2 directions. Hence the only fully determinable components of the Nye tensor are α_{13}, α_{23} and α_{33}. This corresponds to the net Burgers vector of a circuit normal to the sample surface [14]. However, several other components of the Nye tensor can be estimated if strain gradients are neglected in the presence of considerably larger rotation gradients [14]. If all available distortion terms are included in the GND estimate, and the L1 norm (the sum of component absolute values) of the resulting Nye tensor is scaled to compensate for unknown components, a more accurate picture of the GND content can be obtained [17]. Therefore, total GND concentration can be approximated with reasonable accuracy as long as deformation is considered uniform through the sample thickness.

The present work experimentally separates the deformations associated with translation from that associated with rotation, and models mantle deformations as a critical step in accommodating grain boundary sliding creep, in the context of Orowan's classical representation of plastic strain [18]:

$$\gamma = \rho^{(m)} b \bar{x} \tag{2}$$

The plastic shear strain, γ, describes the total number density of mobile dislocations, $\rho^{(m)}$, moving on a slip plane an average distance $\bar{x}$ and b is the Burgers vector. We consider two independent methods for probing the microstructure, particularly understanding the role of the mantle defects in this accommodating step, as distinguished from the grain core behavior. First, deformation mapping using EBSD and improved OIM techniques were employed for spatially quantifying GND densities. To the authors' knowledge, this advanced microscopy technique has not been attempted for quantifying creep deformation structures in ceramics, including these diboride systems. As a second approach, we introduce our version of earlier scribe experiments [19], referred to here as the indentation deformation mapping (IDM) method, which allows for the assessment of grain-to-grain deformation and rotation. The deformations obtained by this IDM method will be interpreted within the context of Orowan's model and the EBSD evidence of dislocation density distributions within the grains.

2. Experimental methods

2.1. Materials and processing

ZrB2–20vol.%SiC billets were produced by Missouri University of Science and Technology (MST). MST billets were hot pressed in a similar manner to that described in Ref. [20]. ZrB_2 powder (Grade B, H.C. Starck, Newton, MA) was >99% pure with average particle size of 2 μm. SiC powder (Grade UF-10, H.C. Starck) was predominantly α-SiC with purity of 98.5% and particle size of 0.7 μm. B_4C/ZrB_2 powder (Grade HD-20, H.C. Starck) was also added to billets at 2 wt.% to reduce SiC/ZrB_2 particle oxide surface films improving densification during pressing. Powders were ball milled with WC–6Co media, resulting in ~2.2–2.4 wt.% WC–6Co impurity concentrations based on true and theoretical density differences. Confirmation of impurity concentration by the X-ray photoelectron spectroscopy analytical technique is reported elsewhere [21]. Additionally, energy dispersive spectroscopy (EDS) confirmed the average W/Zr atomic ratio. A maximum hot pressing temperature and pressure of 1950 °C and 32 MPa, respectively, with heating rates of 30 °C min^{-1} up to 1650 °C and 90 °C min^{-1} up to 1950 °C were employed.